JACC: BASIC TO TRANSLATIONAL SCIENCE VOL. 7, NO. 4, 2022

PRECLINICAL RESEARCH

Genetic Catalytic Inactivation of GRK5 Impairs Cardiac Function in Mice Via Dysregulated P53 Levels

Federica Marzano, PhD,[a] Daniela Liccardo, PhD,[b] Andrea Elia, PhD,[b] Ines Mucio, MS,[b] Claudio de Lucia, MD, PhD,[c] Anna Maria Lucchese, PhD,[c] Erhe Gao, PhD,[c] Nicola Ferrara, MD,[b,d] Antonio Rapacciuolo, MD, PhD,[a] Nazareno Paolocci, MD, PhD,[e,f] Giuseppe Rengo, MD, PhD,[b,d] Walter J. Koch, PhD,[e] Alessandro Cannavo, PhD[b]

VISUAL ABSTRACT

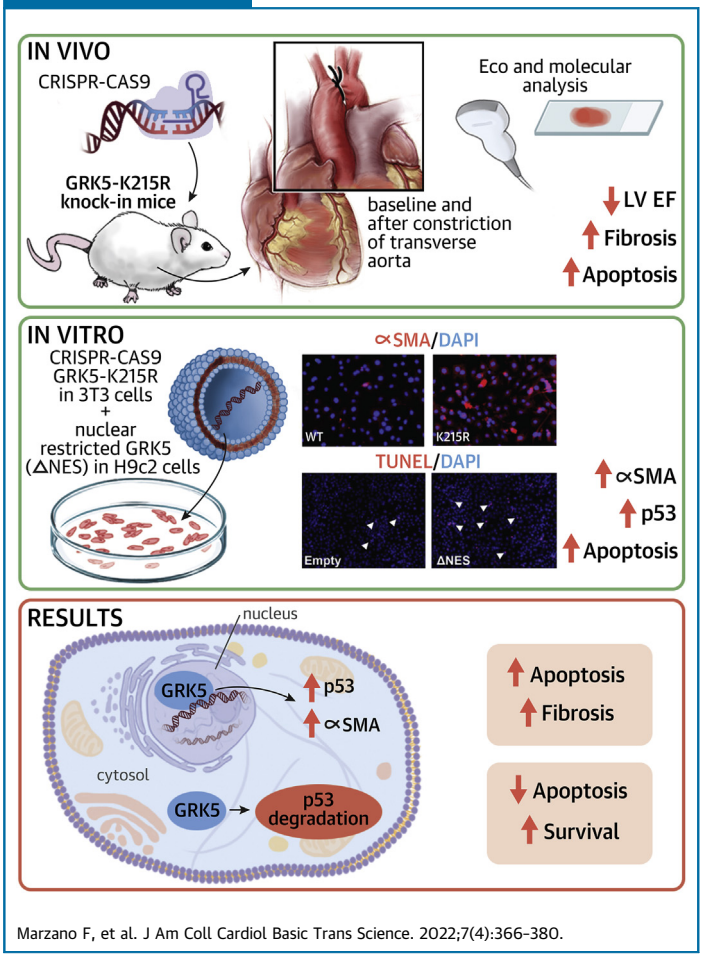

Marzano F, et al. J Am Coll Cardiol Basic Trans Science. 2022;7(4):366–380.

HIGHLIGHTS

- **GRK5 is a major GRK isoform expressed in the heart implicated in HF progression mainly through its noncanonical nuclear activities in myocytes.**
- **This study provides crucial insights into how nuclear GRK5 activity influences myocardial function and response to stress conditions.**
- **GRK5 catalytic activity is essential to preserve cardiomyocyte survival by preventing p53-induced apoptosis and regulating fibroblast activation and cardiac fibrosis.**
- **Overall, these novel effects should be considered when thinking of therapeutic strategies.**

From the [a]Department of Advanced Biomedical Sciences, Federico II University of Naples, Naples, Italy; [b]Department of Translational Medical Sciences, Federico II University of Naples, Naples, Italy; [c]Center for Translational Medicine and Department of Pharmacology, Lewis Katz School of Medicine, Temple University, Philadelphia, Pennsylvania, USA; [d]Istituti Clinici Scientifici ICS-Maugeri, Telese Terme (BN), Italy; [e]Division of Cardiology, Johns Hopkins University Medical Institutions, Baltimore, Maryland, USA; and the [f]Department of Biomedical Sciences, University of Padova, Padova, Italy.

ISSN 2452-302X https://doi.org/10.1016/j.jacbts.2022.01.001

ABSTRACT

GRK5's catalytic activity in regulating basal and stressed cardiac function has not been studied. Herein, we studied knock-in mice in which GRK5 was mutated to render it catalytically inactive (K215R). At baseline, GRK5-K215R mice showed a marked decline in cardiac function with increased apoptosis and fibrosis. In vitro, restriction of GRK5 inside the nucleus of cardiomyocytes resulted in enhanced cell death along with higher p53 levels. Moreover, in fibroblasts, we demonstrated that K215R mutation promoted the transition into myofibroblast phenotype. This study provides novel insight into the biological actions of GRK5, that are essential for its future targeting. (J Am Coll Cardiol Basic Trans Science 2022;7:366–380) © 2022 The Authors. Published by Elsevier on behalf of the American College of Cardiology Foundation. This is an open access article under the CC BY-NC-ND license (http://creativecommons.org/licenses/by-nc-nd/4.0/).

ABBREVIATIONS AND ACRONYMS

GPCR = G protein-coupled receptor

GRK5 = G protein-coupled receptor kinase 5

HDAC5 = histone deacetylase 5

LV = left ventricular

K215R = lysine 215 arginine

NES = nuclear export signal

NLS = nuclear localization signal

PIF = pifithrin

SMA = smooth muscle actin

G protein-coupled receptor kinases (GRKs) are centrally involved in the regulation of critical myocardial receptors such as β-adrenergic receptors (βARs) via phosphorylation, leading to the receptor desensitization and loss of signaling and function.[1] GRK2 expression and activity is markedly up-regulated in the failing human myocardium and critically involved in heart failure (HF) pathogenesis.[1,2] Indeed, GRK2-targeted approaches are emerging amongst the most promising anti-HF therapies.[2] GRK5 is also highly expressed in the heart, is shown to be up-regulated, and is positively associated with human HF.[3,4]

The role of GRK5 is of interest in the heart because of its complex cellular role caused by different compartmentalization. Studies have shown the capability for GRK5 activity to be protective or harmful in the heart, especially after specific stress, and this appears to be caused by specific cellular localization. For example, when confined at the plasma membrane, this kinase displays its canonical effects on specific G protein-coupled receptors (GPCRs), such as βARs, protecting the myocardium against chronic isoproterenol (Iso)-induced cardiac damage.[5] Typically, following β_1AR-phosphorylation, GRK5 recruits β-arrestin and Src to the plasma membrane, leading to metalloproteinase (MMP) activation. MMPs induce the release of the heparin-bound epidermal growth factor and transactivation of EGF receptor (EGFR) and this leads to cardioprotection.[5]

Due to a functional nuclear localization signal (NLS),[6] GRK5 can localize to the nucleus, where our group and others have shown that in cardiomyocytes and fibroblasts, it accumulates after hypertrophic stress.[7–17] Of importance, when GRK5 is elevated in the nucleus of myocytes and fibroblasts, it promotes pathological gene transcription via noncanonical activity, including phosphorylation of histone deacetylase 5 (HDAC5), leading to myocyte enhancing factor 2 (MEF2) de-repression and prohypertrophic and profibrotic gene transcription,[7,12] as well as noncanonical facilitation of nuclear factor of activated T cells (NFAT)-mediated pathological gene transcription,[9] the latter of which may occur in a catalytic-independent manner.[9] Notably, the nuclear accumulation of GRK5 is solely dependent on calcium-calmodulin (Ca^{2+}-CaM) activation,[8,13] and prevention of nuclear localization of GRK5 to stressed myocytes can prevent cardiac pathology.[13]

GRK5 also has noncanonical apoptotic activity involving nuclear and cytosolic targets.[1] In cancer cells and other cell types, such as HEK293, GRK5 can directly bind to and phosphorylate p53 at threonine in position 55, thus determining its degradation and inhibiting the p53-mediated apoptotic response.[18,19] However, GRK5 has been shown to act also as both a proinflammatory and apoptotic enhancer by modulating nuclear NF-kB activity.[14,20,21] Interestingly, both in cardiac and endothelial cells, GRK5 can influence the accumulation and activity of nuclear NF-kB, in a kinase-dependent manner, through the direct phosphorylation of NF-kB, or by its amino-terminal RH domain, via interaction with IκBα.[20,21]

Because some of the previously mentioned evidence appears to involve interactions of GRK5 independent of catalytic activity, it is of interest to

The authors attest they are in compliance with human studies committees and animal welfare regulations of the authors' institutions and Food and Drug Administration guidelines, including patient consent where appropriate. For more information, visit the Author Center.

Manuscript received July 19, 2021; revised manuscript received December 31, 2021, accepted January 3, 2022.

TABLE 1 List of Primers Used for RT-PCR

	Forward	Reverse
Mouse Bnp	CTGAAGGTGCTGTCCCAGAT	CCTTGGTCCTTCAAGAGCTG
Mouse Bax	AAACTGGTGCTCAAGGCCC	CTTGGATCCAGACAAGCAGC
Mouse Apaf-1	TCCCTGGGCTGCTTTCTTTC	CCGGATGTGTAACCAAGCCT
Mouse Caspase3	GATCCTTTGTGTTGCCTCCAG	TGGTCACTTTTCTTAGCCAGGTT
Mouse p53	ATTCAGGCCCTCATCCTCCT	CCATGGCAGTCATCCAGTCT
Rat p53	GGTACCGTATGAGCCACCTG	GACAGGCACAAACACGAACC
Mouse/Rat 18S	TCAAGAACGAAAGTCGGAGG	GGACATCTAAGGGCATCAC

RT-PCR = reverse transcription - polymerase chain reaction.

specifically target this activity to attempt to determine whether phosphorylation mediated from GRK5 in the heart is liable for these undesired prohypertrophic effects, or if it is instead involved in the protective ones, such as countering apoptosis. We sought to solve these issues by creating and developing a novel knock-in line of mice expressing a catalytically inactive form of GRK5 (GRK5-lysine 215 arginine [K215R]). We characterized the cardiac phenotype of these mice basally and after ventricular pressure overload and HF development. Our results reveal clear connections between the catalytic activity of GRK5 in the nucleus and p53-mediated apoptosis and fibrosis that has profound effects on cardiac function and the heart's response to stress.

METHODS

ANIMAL MODELS. All animal procedures were performed according to the Institutional Animal Care and Use Committee of Temple University Lewis Katz School of Medicine guidelines. We used wild-type (WT) mice and GRK5-K215R knock-in mice.

GENERATION OF GRK5-K215R KNOCK-IN MICE USING THE CRISPR/CAS9 TECHNOLOGY. We used the CRISPR/Cas9 system to generate a specific mutation, in exon 8 of the gene coding for this kinase, of the AAA triplet Coding for lysine (K) in position 215. Using a specific online available software,[22] we identified a single guide RNA in the vicinity of the sequence to be mutated that was inserted into a specific vector, using the restriction enzyme BbsI (Addgene Plasmid #42230; pX330-U6-Chimeric_BB-CBh-hSpCas9, modified by inserting EF1alpha-EGFP fragment to visualize their expression in cells). Subsequently, we used a homology direct repair approach. To this end, we designed and used a single-stranded oligonucleotide of 90 BP on the right arm and 90 BP on the left arm ('5'- ACATCTGTAGTATGCTATGACCTGAGTATCTCCCTTCTACCGCAGGTCTGTGCCTGCCAGGTTCGGGCCACTGGTAAAATGTATGCTTGTCGACGCTTAGAGAAGAAGAGAATCAAAAAGAGGAAAGGCGAATCCATGGCACTCAACGAAAAGCAGATTCTTGAGAAGGTCAACAGCCAGTTTGTGGTGAGTGTCCAGGG-3'). Murine cells (3T3) were cotransfected with 1 μg of plasmid containing the guide RNA and with 2 μmol/L of ssODN, using the Lipofectamine reagent 2000 (Invitrogen). To generate the knock-in mice, the plasmid and the ssODN were injected directly into the mouse egg pronucleus. Once identified, the animals carrying the mutation were used to establish a colony of homozygous mice K215R.

IN VIVO EXPERIMENTAL PROCEDURES. As previously reported, pressure overload in mice was performed by constriction of the transverse aorta (TAC).[11] Briefly, before surgery, WT and GRK5-K215R (9-week-old) mice were anesthetized with isoflurane (induction 3% and maintenance 1.5%). Subsequently, they were intubated, and a cervical incision was performed on the midline to expose the trachea and carotid arteries. Next, a 20-gauge blunt needle was inserted into the trachea and connected to a mechanical ventilator (volume-cycle rodent fan with Supplemental oxygen) at a rate of 1 L/min and respiratory rate of 140 breaths/min. Next, the aortic constriction was performed by tying a nylon suture wire (7-0) to a 27-mm needle. The latter was promptly removed to obtain a constraint of 0.4 mm in diameter. Sham-operated mice were used as a control. After 4 weeks, transthoracic echocardiography was performed, and the mice were sacrificed. Then, cardiac specimens were excised, weighed, and used for biochemical and histological analysis.

ECHOCARDIOGRAPHY. All animals (WT and K215R) used in this study were subjected to 2-dimensional transthoracic echocardiography and M-mode in basal conditions and 4 weeks after TAC. As previously described, this analysis was performed in mice with a VEVO 2100 echocardiograph (Visualsonics) with a MS400 (30-MHz centerline frequency) probe. The measured echocardiographic parameters were as follows: left ventricular end-diastolic diameter (LVEDd) (mm); left ventricular end-systolic diameter (LVESd) (mm); telesystolic dimension percentage of the left ventricle fractional shortening (FS) (FS = LVEDd - LVESd/LVEDd %); and percentage of ejection fraction (EF%).

HISTOLOGY. Cardiac samples were fixed in 4% formaldehyde and embedded in paraffin. Subsequently, the samples were cut in 4-μm-thick sections with microtome and mounted on glass slides.

Fibrosis. To evaluate the percentage of interstitial fibrosis after deparaffinization and hydration in decreasing alcoholic series, the cardiac sections were stained by incubation for 1 hour with Red Picro-Sirio.

FIGURE 1 GRK5-K215R Mutation Negatively Affects Basal Cardiac Function and Fibrosis in Vivo in Mice

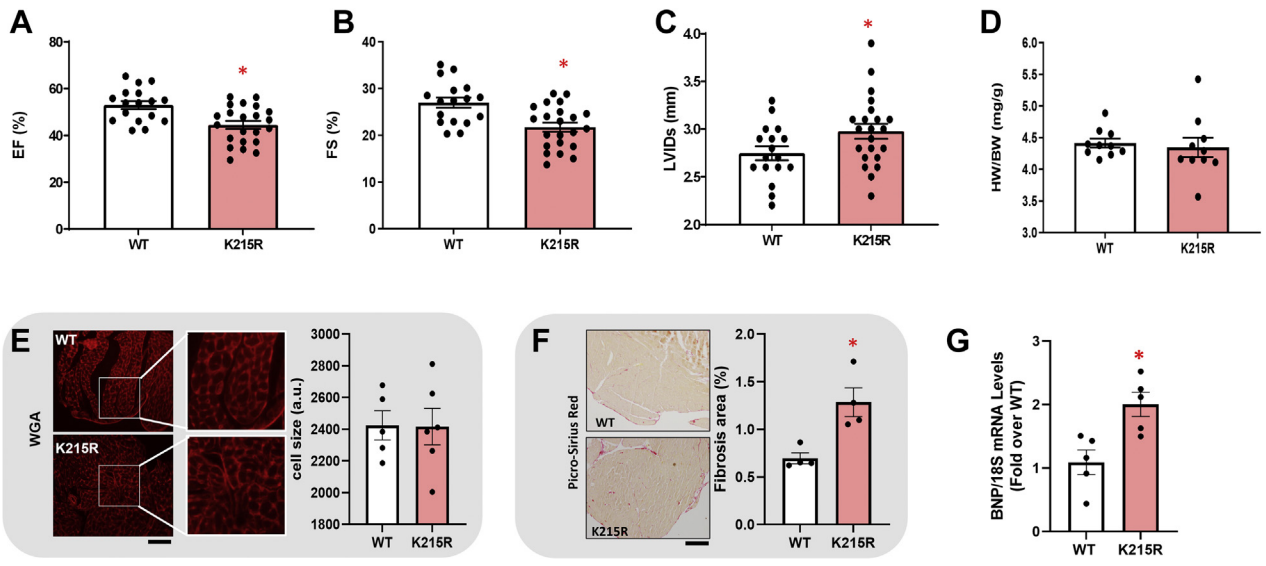

(A-C) Scatter plot with bar graph showing echocardiographic analysis of **(A)** left ventricular (LV) ejection fraction (EF) (%), **(B)** fractional shortening (FS) (%), and **(C)** left ventricular internal diameter in systole (LVIDs) of individual mice from the wild type (WT) and GRK5 K215R groups. **(D)** Scatter plot with bar graph showing heart weight (HW) and body weight (BW) ratio in WT and K215R groups of mice. **(E)** Representative panels **(left)** and quantitative analysis **(right)** showing myocyte cell size (WGA staining, scale bar 100 μm) in cardiac sections from WT and GRK5-K215R mice. **(F)** Representative images **(left)** and quantitative data **(right)** showing percentage of cardiac fibrosis (Picro-Sirius red staining, scale bar 100 μm) in WT and GRK5-K215R mice. **(G)** Scatter plot with bar graph showing mRNA levels of B-type natriuretic peptide in total LV lysates from WT and GRK5-K215R group of mice. 18S rRNA was used as internal control gene. 2-tailed unpaired Student's *t-test*: $*P < 0.05$ vs WT. All data are shown as mean ± SEM.

Finally, the slices were dehydrated after staining by a passage in absolute ethanol and xylene and were mounted for viewing under a microscope with an assembly medium (Eukitt). For each histological section, 5-6 images were acquired using a motic BA410 microscope. The percentage of the fibrotic area was calculated using the ImageJ software.

Hypertrophy. To evaluate cardiac hypertrophy, we performed staining with wheat germ agglutinin. Each histological section of 5-6 images were acquired using a ZOE Fluorescent Cell Imager Microscope (Bio-Rad Laboratories). The percentage of cell hypertrophy was calculated using the ImageJ software.

Apoptosis. To assess the effects on cell death, we performed a TUNEL assay (terminal deoxynucleotidyl transferase [TDT]-mediated dUTP Nick end labeling) on cells or on fixed paraffin-embedded left ventricular (LV) sections, using a commercial kit (Roche). The assay was performed according to the manufacturer's instructions. After staining, the sections were incubated with the DAPI fluorescent dye (Sigma-Aldrich). Next, 5-6 images were acquired for each sample using ZOE Fluorescent Cell Imager Microscope (Bio-Rad Laboratories). Then, the percentage of apoptotic cells was calculated using the ImageJ software, by evaluating the percentage of cells colored with DAPI and positive to TUNEL.

WESTERN BLOT ANALYSIS. Cells (neonatal rat ventricular myocytes) and LV specimens were rinsed in phosphate-buffered saline and then lysed in RIPA buffer (Tris-HCl, pH 7.5; NaCl, 1%; Nonidet P-40, 0.5%) with protease (cOmplete-Roche) and phosphatase inhibitors (PhosSTOP-Roche). The protein content was quantized using a DC Protein Assay (Bio-Rad) and read at 750 nm using a Multiskan FC Microplate Photometer (Thermo Scientific). The proteins (30 μg) were separated by SDS-PAGE using gradient 4%-20% precast gels (Thermo Fisher Scientific) and then were transferred to a PVDF membrane (Bio-Rad). Milk (5%) dissolved in TBS buffer containing tween 20 (0.01%) was used to block nonspecific sites. After blocking, the membranes were incubated overnight at 4 °C with the primary antibody. Then, the proteins were probed with a corresponding secondary antibody and visualized with a

FIGURE 2 GRK5-K215R Mutation Impairs Cardiac Cells Survival in Vivo

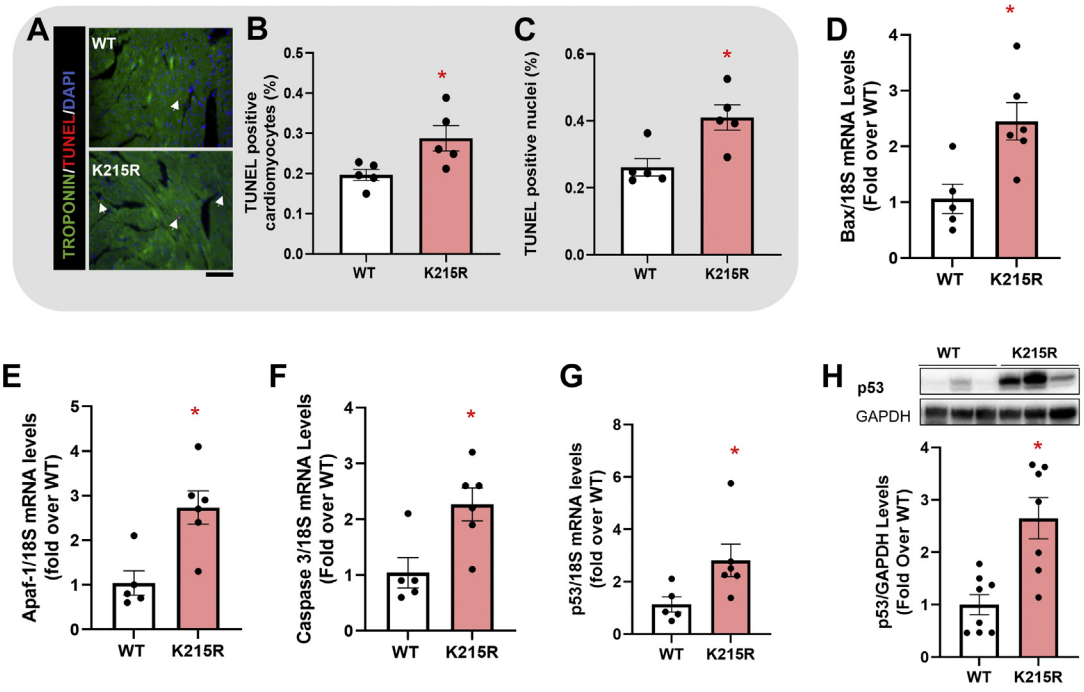

(A-C) Representative panels **(A)** and quantitative analysis showing percentage of TUNEL positive cardiomyocytes **(B)** and TUNEL positive cells **(C)** (TUNEL/DAPI staining, scale bar 50 μmol/L). LV sections were counterstained with Troponin T **(green)** to visualize cardiomyocytes. **(D-G)** Scatter plot with bar graph showing mRNA levels of **(D)** Bax, **(E)** Apaf-1, **(F)** Caspase 3, and **(G)** p53 in total LV lysates from WT and GRK5-K215R group of mice. 18S rRNA was used as internal control gene. **(H)** Representative immunoblots **(top)** and densitometric quantitative analysis **(bottom)** of multiple independent experiments to evaluate p53 levels in total LV lysates from WT and GRK5-K215R group of mice. glyceraldehyde-3-phosphate dehydrogenase was used as loading control. 2-tailed unpaired Student's *t-test*: $*P < 0.05$ vs WT. All data are shown as mean ± SEM. Abbreviations as in Figure 1.

chemi-doc XRS system (Bio-Rad). Quantitative densitometric analysis was performed using the chemi-doc XRS imaging software. The following primary antibodies were used: p53 (10442-1-AP, Proteintech, 1:1,000); glyceraldehyde-3-phosphate dehydrogenase (SC-32233, 6c5; Santa Cruz Biotechnology, 1:2,000); Cleaved Caspase-3 (#9661, Cell Signaling, 1:1,000); phospho-NF-kB p65 (#3033, Cell Signaling, 1:1,000); NF-kB p65 (#6956, Cell Signaling, 1:1,000); GRK5 (ab64943, Abcam, 1:1,000); Fibrillarin (ab5694, Abcam, 1:1,000); and α-smooth muscle actin (αSMA) (ab5694, abcam; 1:1,000).

REAL-TIME PCR. According to the company's instructions, total RNA was isolated from H9c2 cells and LV specimens with TRIzol (Thermo Fisher Scientific). After RNA isolation, cDNA was synthesized by reverse transcription of the RNA (iScript cDNA synthesis kit, Bio-Rad Laboratories). Real-time PCR was performed on a StepOne Real-Time PCR System (Applied Biosystems) using the Power SYBR Green PCR Master Mix (Applied Biosystems) and specific primers for rat and mouse gene of interest (Table 1). The expression levels of these genes were normalized to 18S rRNA. The specificity of PCR products was confirmed by melting curve and gel electrophoresis.

CELL CULTURE AND STIMULATION. H9c2 myoblasts were purchased from Sigma-Aldrich (88092904) and 3T3 fibroblasts were purchased from ATCC (ATCC CL-1658). Both cell lines were cultured in Dulbecco's Modified Eagle Medium supplemented with 10% fetal bovine serum (FBS) and 1% P/S.

3T3 were stimulated with Iso (10 μmol/L, I6504 Sigma-Aldrich) for 10 minutes. Unstimulated cells were used as controls.

Moreover, a group of cells (both 3T3 and H9c2) was pretreated with pifithrin-α (PIFα) (20 μmol/L; S2929, selleckchem) for 2 h in serum free medium and then maintained in medium supplemented with 0.5% FBS for 24h.

FIGURE 3 **Depletion of GRK5 Catalytic Activity Accelerates the Onset of HF After Pressure-Overload in Mice**

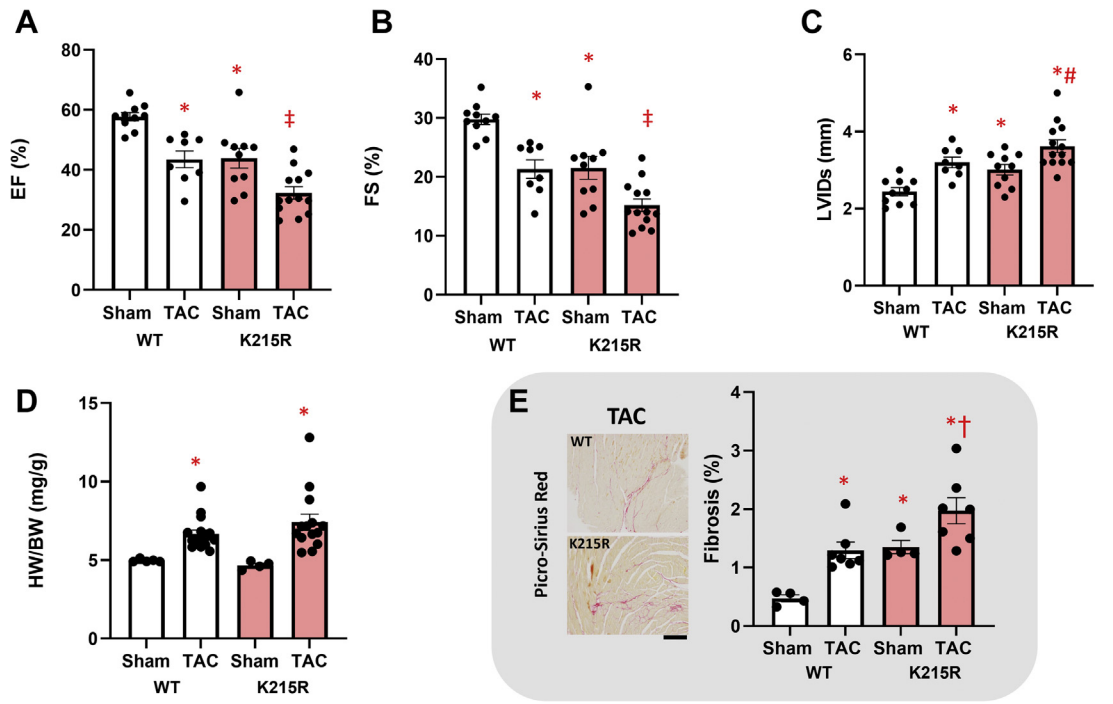

(A-C) Scatter plot with bar graph showing echocardiographic analysis of **(A)** LV EF (%), **(B)** FS (%), and **(C)** LVIDs of individual mice from the WT and GRK5 K215R groups (Sham and TAC). **(D)** Scatter plot with bar graph showing HW and BW ratio in WT and K215R groups of mice. **(E)** Representative images **(left)** and quantitative data **(right)** showing percentage of cardiac fibrosis (Picro-Sirius red staining, scale bar 100 μm) in WT and GRK5 K215R mice (Sham and TAC). Analysis of variance with Tukey's multiple comparisons post hoc test: *$P < 0.05$ vs WT sham; #$P < 0.05$ vs K215R sham; †$P < 0.05$ vs WT TAC; ‡$P < 0.05$ vs all. All data are shown as mean ± SEM. Abbreviations as in Figure 1.

ADENOVIRUS TRANSDUCTION. H9c2 cells were plated in a 6-well multiwell dish and infected with recombinant, replication-deficient adenoviruses expressing GFP (50 multiplicity of infection [MOI]), GRK5-ΔNLS (50 MOI), GRK5 (50 MOI), LacZ (50 MOI), and Gq-CaM (50 MOI). Cells were cultured for 24 hours before experimentation.

PLASMID TRANSFECTION. To evaluate the effect of GRK5 nuclear localization, H9c2 cells were transfected with 2 μg of plasmid expressing GRK5- ΔNES (a mutated version of GRK5 without its nuclear export signal [NES]), using the Lipofectamine reagent 2000 (Invitrogen). Cells were cultured for 24 hours before experimentation. The 3T3 cell line expressing GRK5-K215R was generated as described in the previous text and used for experimentation.

IMMUNOFLUORESCENCE. 3T3 fibroblasts, either WT or stable expressing GRK5-K215R mutation and H9c2 cells, overexpressing GRK5-WT, GRK5-ΔNLS, and GRK5-ΔNES, were fixed in 4% PFA for 10 minutes and then washed 3 times in ice cold phosphate-buffered saline and permeabilized with 0.2% Triton X-100. Then, 3T3 and H9c2 were incubated with 1% BSA for 30 min and incubated overnight at 4 °C with an anti-αSMA (ab5694, abcam; 1:200) or with an anti-GRK5 antibody (ab64943, Abcam, 1:200), respectively. Next, cells were incubated with the respective secondary antibodies (1:200). After staining, the sections were incubated with the DAPI fluorescent dye (Sigma-Aldrich). Images were acquired using ZOE Fluorescent Cell Imager Microscope (Bio-Rad Laboratories).

NUCLEAR EXTRACTION. Nuclear fractions were obtained from 3T3 fibroblasts, either WT or expressing GRK5-K215R mutation. Cells were lysed in Buffer A (10 mmol/L 4-[2-hydroxyethyl]-1-piperazineethanesulfonic acid [HEPES], pH 7.9; 10 mmol/L KCl; 0.1 mmol/L EDTA [EDTA]) to isolate nuclei, supplemented with octylphenoxypolyethoxyethanol and protease inhibitors. Lysate was then centrifuged at 13,000 × *g* for 10 minutes at 4 °C. The supernatant was transferred to a new tube (cytosolic fraction), whereas the pellet containing the nuclei fraction was resuspended in fresh prepared buffer B (20 mmol/L HEPES, pH 7.9; 0.4 mol/L NaCl; 1 mmol/L

FIGURE 4 The GRK5 Mutant Lacking ΔNLS Blunts P53 Expression in H9c2 Cardiomyocytes

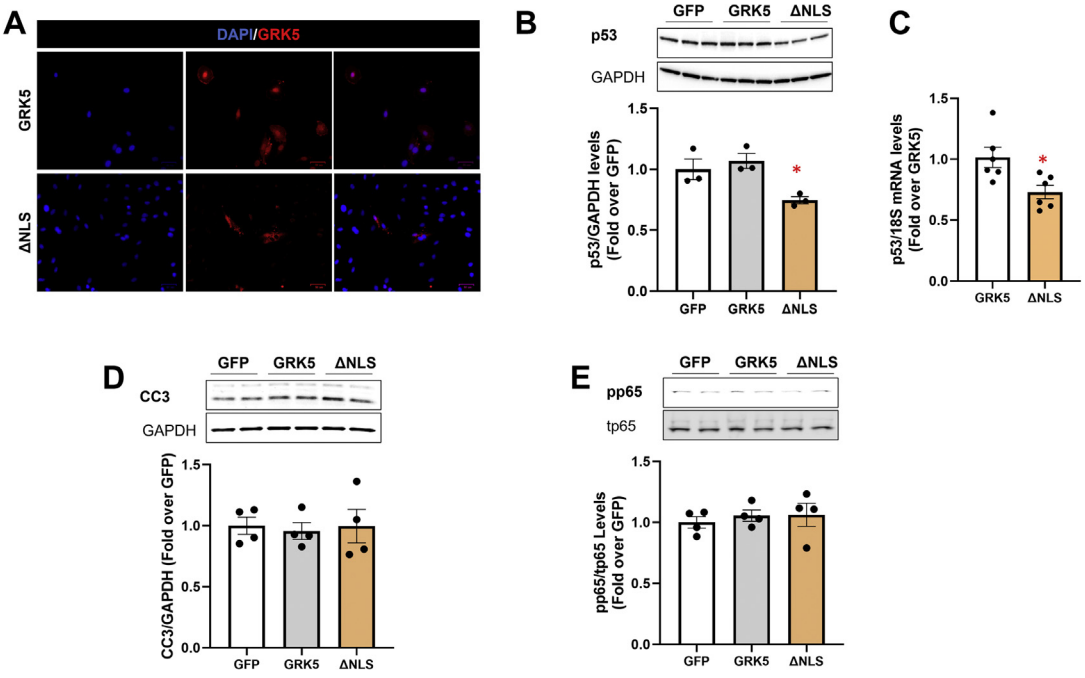

(A) Representative immunofluorescence staining of H9c2 cells infected with Adenoviruses (Ad) encoding for WT-GRK5 and a mutant form of GRK5-nuclear localization signal (ΔNLS). Cells were stained with Ab to GRK5 **(red)** to show GRK5 subcellular distribution. Nuclei were counterstained with DAPI **(blue). (B)** Representative immunoblots **(top)** and densitometric quantitative analysis **(bottom)** of multiple independent experiments to evaluate p53 levels in H9c2 cells overexpressing GFP, GRK5, and GRK5-ΔNLS. Glyceraldehyde-3-phosphate dehydrogenase was used as loading control. Analysis of variance with Tukey's multiple comparisons post hoc test: $*P < 0.05$ vs GFP. **(C)** Scatter plot with bar graph showing mRNA levels of p53 in H9c2 cells overexpressing GRK5 and GRK5-ΔNLS. 18S rRNA was used as internal control gene. 2-tailed unpaired Student's *t-test*: $*P < 0.05$ vs GRK5. **(D)** Representative immunoblots **(top)** and densitometric quantitative analysis **(bottom)** of multiple independent experiments to evaluate CC3 levels in H9c2 cells overexpressing GFP, GRK5, and GRK5-ΔNLS. Glyceraldehyde-3-phosphate dehydrogenase was used as loading control. **(E)** Representative immunoblots **(top)** and quantitative data **(bottom)** showing phosphorylation levels of p65 as a ratio of activated p65 (pp65) to total p65 (tp65) in H9c2 cells overexpressing GFP, GRK5, and GRK5-ΔNLS. All data are shown as mean ± SEM.

EDTA; 10% glycerol; protease inhibitors), shacked for 2 hours, and, finally, centrifuged at 13,000 × *g* for 5 minutes at 4 °C. The supernatant was directly used for protein quantification and immunoblotting.

DNA BINDING ASSAY. 3T3 cells were lysed in a lysis buffer (10 mmol/L HEPES, pH 7.4, 0.1% Triton X-100, 0.1 M NaCl, 10% glycerol, and 0.05 mmol/L EDTA supplemented with protease inhibitors) and centrifugated at 13,000 × *g* for 20 minutes. Then, cell lysates (300 μg) were incubated with 25 μL of single-stranded DNA-cellulose (D8273, Sigma Aldrich) in 100 μL of cold binding buffer (10 mmol/L HEPES [pH 7.4], 1 mmol/L $MgCl_2$, 0.1% Triton X-100, 3 mmol/L dithiothreitol, 0.1 mol/L NaCl, 0.05 mmol/L EDTA) for 1 hour at 4°C, as previously described.[6]

Following incubation, the resin was washed 4 times with 1 mL of binding buffer by using Poly-Prep Chromatography Columns (#7311550, Bio-Rad) and then eluted with elution buffer. The amount of protein retained on the resin was determined by Western blot analysis.

STATISTICAL ANALYSIS. Data are expressed as the mean ± SEM. Comparisons of 2 groups were done using Student's *t-test*. Three or more groups were compared using 1-way analysis of variance followed by Dunnett's or Tukey's post hoc test for multiple pairwise comparisons. All data were analyzed using GraphPad Prism software version 9.1 (GraphPad Software). A P value < 0.05 was considered statistically significant.

RESULTS

GENERATION OF KINASE-DEAD GRK5-K215R KNOCK-IN MUTANT MICE. To determine the overall

FIGURE 5 **Nuclear Accumulation of GRK5 Increases p53 Expression and Cell Death Rate in H9c2 Cardiomyocytes In Vitro**

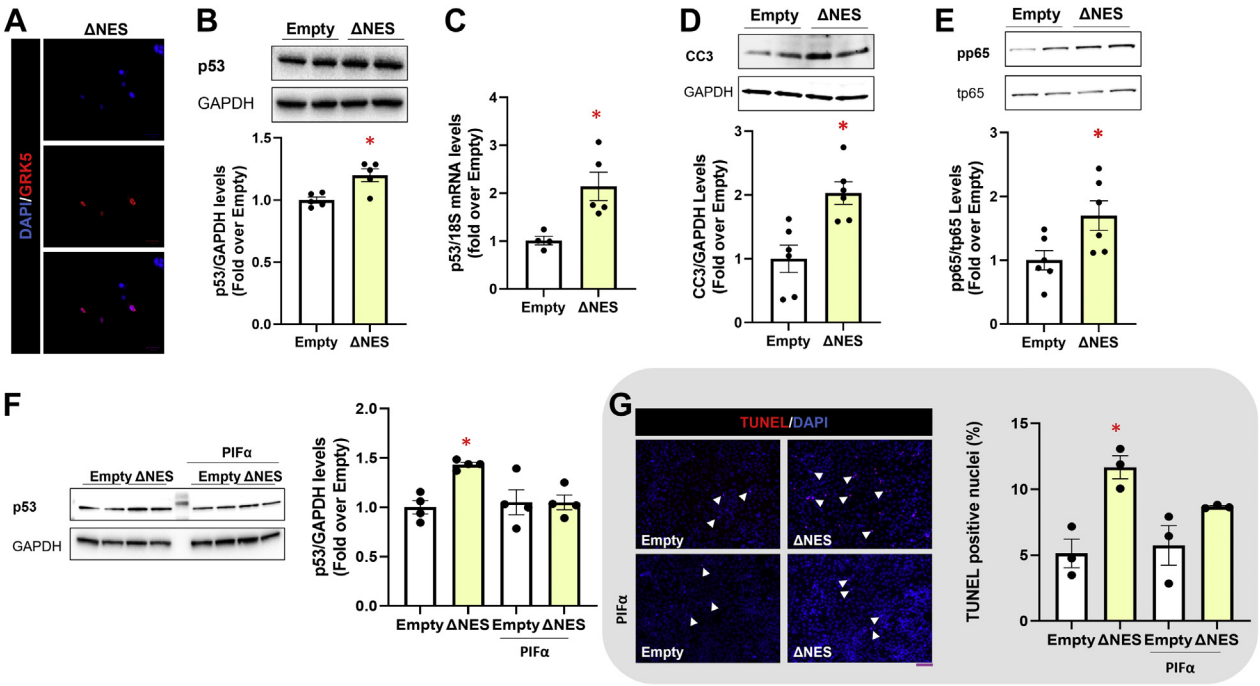

(A) Representative immunofluorescence staining of H9c2 cells transfected with the mutant form of GRK5 lacking the nuclear export signal (GRK5-ΔNES). Cells were stained with Ab to GRK5 **(red)** to show GRK5 subcellular distribution. Nuclei were counterstained with DAPI **(blue). (B)** Representative immunoblots **(top)** and densitometric quantitative analysis **(bottom)** of multiple independent experiments to evaluate p53 levels in H9c2 cells transfected with an empty vector or GRK5-ΔNES. Glyceraldehyde-3-phosphate dehydrogenase was used as loading control. **(C)** Scatter plot with bar graph showing mRNA levels of p53 in H9c2 cells transfected with an empty vector or GRK5-ΔNES. 18S rRNA was used as internal control gene. **(D)** Representative immunoblots **(top)** and densitometric quantitative analysis **(bottom)** of multiple independent experiments to evaluate CC3 levels in H9c2 cells transfected with an empty vector or GRK5-ΔNES. Glyceraldehyde-3-phosphate dehydrogenase was used as loading control. **(E)** Representative immunoblots **(top)** and quantitative data **(bottom)** showing phosphorylation levels of p65 (pp65/tp65) in H9c2 transfected with an empty vector or GRK5-ΔNES. 2-tailed unpaired Student's *t-test*: $*P < 0.05$ vs empty. **(F)** Representative immunoblots **(top)** and densitometric quantitative analysis **(bottom)** of multiple independent experiments to evaluate p53 levels in H9c2 cells transfected with an empty vector or GRK5-ΔNES. The cells were either unstimulated or treated with the p53 inhibitor Pifithrin-α (PIFα) (20 μmol/L) for 2 h and then maintained in medium supplemented with 0.5% FBS for 24h. Glyceraldehyde-3-phosphate dehydrogenase was used as loading control. **(G)** Representative panels **(left)** and quantitative analysis **(right)** showing percentage of cell death (TUNEL/DAPI staining, scale bar 100 μmol/L) in H9c2 cells expressing an empty plasmid or GRK5-ΔNES. The cells were either unstimulated or treated with the p53 inhibitor PIFα (20 μmol/L) for 2 hours and then maintained in medium supplemented with 0.5% FBS for 24 hours. Analysis of variance with Dunnett's multiple comparisons post hoc test: $*P < 0.05$ vs empty. All data are shown as mean ± SEM.

significance of the catalytic activity of GRK5, we used CRISPR/Cas9 technology to generate a specific mutation of the ATP binding lysine (K215) within the catalytic site of GRK5 and replaced this with an arginine (R). This mutation (GRK5-K215R) causes the complete loss of kinase activity of GRK5, as previously reported.[23] GRK5-K215R mice were generated, and WT littermates and mutant lines were colonized as previously done for a different mutant knock-in line by our laboratory.[24] We confirmed the K215R mutation in mice by RFLP analysis and sequencing (Supplemental Figures 1A and 1B). Finally, we analyzed the total protein levels of GRK5, by immunoblot, in cardiac tissue of WT and K215R mice. As expected, no difference in GRK5 expression was observed, thus confirming that the mutation did not affect GRK5 expression in the heart (Supplemental Figure 1C). Because these animals are a global knock-in, the expression of GRK5 was also checked in noncardiac tissues such as the brain, into which GRK5 is expressed at high levels,[19] and this was also shown to be unchanged (Supplemental Figure 1D).

Next, to verify that the mutation abolished the catalytic activity of GRK5 functionally, a group of animals was injected (intraperitoneally) with the βAR-agonist Iso (1 mg/kg). In contrast, the control group was treated only with vehicle (water). Fifteen minutes after Iso administration, animals were

FIGURE 6 GRK5-K215R Mutation Increased GRK5's DNA-Binding Ability and the Apoptotic Response in Fibroblasts in Vitro

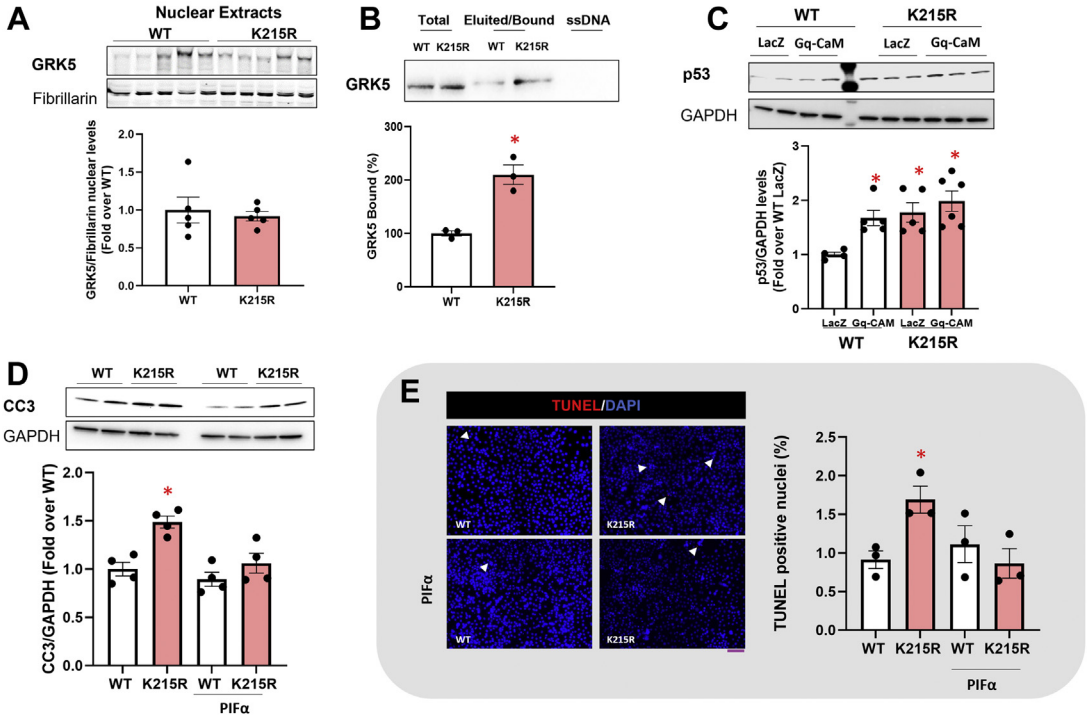

(A) Representative immunoblots **(top)** and densitometric quantitative analysis **(bottom)** of multiple independent experiments to evaluate GRK5 levels in nuclear extracts purified from both 3T3 cells WT and stable expressing GRK5-K215R mutant. Fibrillarin was used as loading control. **(B)** Representative immunoblots **(top)** and densitometric quantitative analysis **(bottom)** of multiple independent experiments to evaluate the percentage of GRK5 bound to DNA in 3T3 cells (WT-GRK5 vs stable expressing GRK5-K215R mutant). **(C)** Representative immunoblots **(top)** and densitometric quantitative analysis **(bottom)** of multiple independent experiments to evaluate p53 levels in 3T3 cells, either WT or expressing GRK5-K215R mutation. Cells were also infected with Adenoviruses (Ad) encoding for LacZ or Gq-CaM. Glyceraldehyde-3-phosphate dehydrogenase was used as the loading control. Analysis of variance with Tukey's multiple comparisons post hoc test: $^*P < 0.05$ vs WT. **(D)** Representative immunoblots **(top)** and densitometric quantitative analysis **(bottom)** of multiple independent experiments to evaluate CC3 levels in 3T3 cells WT and stable expressing GRK5-K215R mutant. The cells were either unstimulated or treated with the p53 inhibitor PIFα (20 μmol/L) for 2 hours and then maintained in medium supplemented with 0.5% FBS for 24h. Glyceraldehyde-3-phosphate dehydrogenase was used as loading control. **(E)** Representative panels **(left)** and quantitative analysis **(right)** showing percentage of cell death (TUNEL/DAPI staining, scale bar 100 μmol/L) in 3T3 cells WT and stable expressing GRK5-K215R mutant. The cells were either unstimulated or treated with the p53 inhibitor PIFα (20 μmol/L) for 2 hours and then maintained in medium supplemented with 0.5% FBS for 24 hours. Analysis of variance with Dunnett's multiple comparisons post hoc test: $^*P < 0.05$ vs WT. All data are shown as mean ± SEM. Abbreviations as in Figure 1.

sacrificed, and the hearts were excised for immunoblot analysis. Notably, while in WT mice, Iso induced a significant rise in EGFR phosphorylation and ERK activation (pERK), as previously shown to be GRK5-dependent[5] (Supplemental Figures 2A to 2C), the lack of GRK5 kinase activity completely abolished the βAR-dependent transactivation of EGFR (Supplemental Figures 2A to 2C).

GRK5-K215R MICE DISPLAY BASAL CARDIAC DYSFUNCTION. Next, we sought to determine whether the lack of GRK5 kinase activity would affect cardiac function and LV geometry at baseline. Although the K215R animals entered adult life in apparent healthy status, echocardiographic analysis performed at 9-10 weeks of age (a time point typically chosen for surgical procedures[10]) revealed a statistically significant deterioration of cardiac function, expressed as changes in the %EF and %FS, compared with age-matched WT animals (**Figures 1A and 1B**). An early time point (4 weeks of age) was also evaluated, and we observed a similar cardiac dysfunction degree compared with the adult counterparts (Supplemental Figure 3). Interestingly, all mutant mice displayed increased LV end-diastolic diameters, denoting

FIGURE 7 GRK5-K215R Mutation Promotes the Transition of Fibroblasts Into Myofibroblasts in Vitro

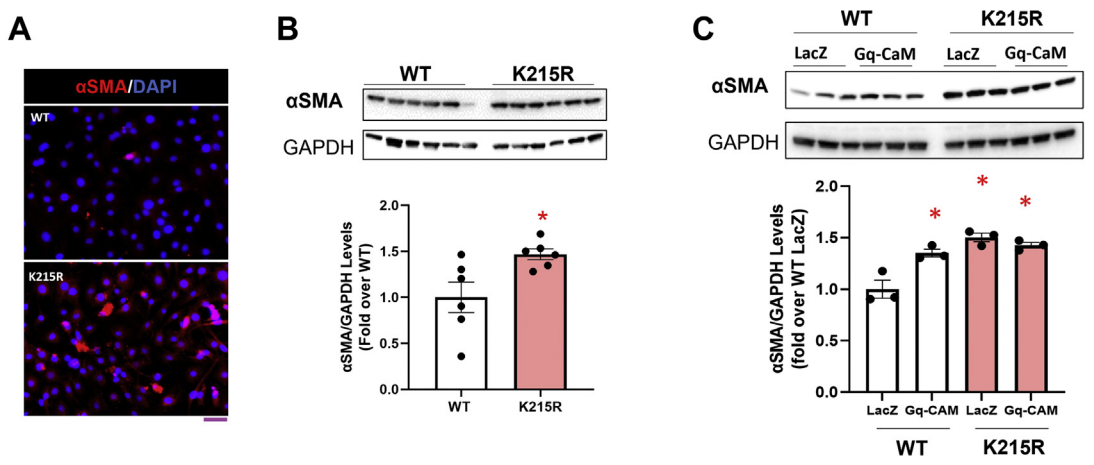

(A) Representative immunofluorescence of 3T3 cells WT and stable expressing GRK5-K215R mutant, stained for α-smooth muscle actin (αSMA) **(red)** and cell nuclei (DAPI, **blue**). Scale bar, 50 μm. **(B)** Representative immunoblots **(top)** and densitometric quantitative analysis **(bottom)** of multiple independent experiments to evaluate αSMA levels in 3T3 cells either WT or stable expressing GRK5-K215R mutant. Glyceraldehyde-3-phosphate dehydrogenase was used as loading control. 2-tailed unpaired Student's *t-test*: $*P < 0.05$ vs WT. **(C)** Representative immunoblots **(top)** and densitometric quantitative analysis **(bottom)** of multiple independent experiments to evaluate αSMA levels in 3T3 cells either WT or stable expressing GRK5-K215R mutant. Cells were also infected with Adenoviruses (Ad) encoding for LacZ or Gq-CaM. Glyceraldehyde-3-phosphate dehydrogenase was used as loading control. Analysis of variance with Tukey's multiple comparisons post hoc test: $*P < 0.05$ vs WT. All data are shown as mean ± SEM. Abbreviations as in Figure 1.

constitutive LV chamber dilation (Figure 1C). Of note, this basal LV phenotype persisted over time without affecting the survival of K215R mutant mice under basal (unstressed) conditions. Surprisingly, GRK5-K215R knock-in mice did not show significant cardiac hypertrophy compared with WT control subjects, as demonstrated by heart weight and body weight ratios (Figure 1D).

GRK5-K215R MICE PRESENT WITH INCREASED INTERSTITIAL FIBROSIS AND APOPTOSIS. We next assessed myocyte size to determine whether the gene-editing of GRK5 kinase activity alters cardiac mass or morphology. Compared with WT control subjects, GRK5-K215R mutant mice did not show any difference in cardiomyocyte cell size as per wheat germ agglutinin staining (Figure 1E). However, cardiac samples from mutant mice displayed prominent cardiac fibrosis (Figure 1F) and increased B-type natriuretic peptide mRNA levels (Figure 1G). This is consistent with previous studies showing that in patients with cardiomyopathy[25] and in mice,[26] cardiac fibrosis is associated with increased B-type natriuretic peptide secretion and cardiac expression.[25,26] Next, we analyzed the effects of K215R mutation on cardiac apoptosis. In particular, we performed a TUNEL staining on cardiac sections from WT and mutant mice. To differentiate cardiomyocytes specifically, we counterstained the sections with troponin T. As shown in Figure 2A, K215R mutation negatively affected cardiomyocytes and whole cardiac cells' survival. Indeed, the apoptotic rates in GRK5-K215R hearts were significantly higher than those of WT (Figures 2B and 2C). Furthermore, we analyzed the expression levels of different proapoptotic genes, including Bax, Apaf-1, Caspase-3, and p53, which were all up-regulated in K215R hearts compared with their WT counterparts (Figures 2D to 2G). Because p53 is a well-recognized proapoptotic target regulated by GRK5, we evaluated the effects of K215R mutation on p53 protein levels in cardiac and noncardiac tissues (brain tissue). As shown in Figure 2H (cardiac tissue) and in Supplemental Figure 4 (brain tissue), p53 was up-regulated in both tissues of K215R mice compared with those of WT animals. However, only in the heart was this increase in p53 protein levels statistically different between the 2 experimental groups. Notably, the current evidence corroborates previous observations suggesting that GRK5's kinase activity can inhibit p53 protein levels,[18,27] while providing new evidence for a potential role in its transcriptional regulation that is mostly kinase independent. In this regard, as shown in Supplemental Figure 5, our RT-PCR data confirmed previous observation[9] showing that GRK5, in a kinase-independent manner, may

FIGURE 8 Schematic Representation of GRK5 Activities in Cardiomyocytes

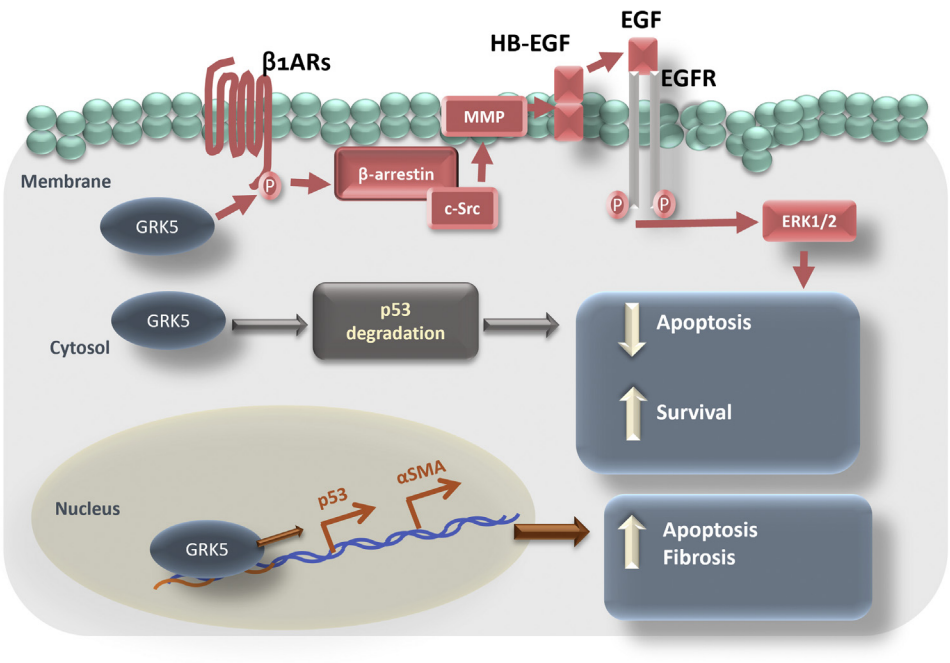

When at the plasma membrane, GRK5 regulates the function of several GPCRs, including beta-adrenergic receptors (βARs). Following β1ARs phosphorylation, GRK5 recruits β-arrestin and Src to the plasma membrane, leading to metalloproteinase (MMP) activation and release of the heparin-bound epidermal growth factor (HB-EGF), which transactivate EGF receptor (EGFR) and promote prosurvival signaling. When in the cytosol and nuclei, GRK5 directly controls p53 expression/activity by controlling its degradation. In the nuclei and through direct DNA-binding, GRK5 increases p53 and αSMA expression, thus inducing cardiomyocyte cell death and fibrosis.

activate transcription factor-like NFAT, leading to the up-regulation of downstream prohypertrophic or apoptotic genes (eg, regulator of calcineurin 1).

GRK5-K215R MICE HAVE HEIGHTENED LOSS OF CARDIAC FUNCTION IN RESPONSE TO LV PRESSURE OVERLOAD STRESS. Next, we modeled chronically elevated LV afterload conditions in mice via TAC to assess the effects of the lack of GRK5 catalytic activity after stress. To this purpose, both WT and GRK5-K215R mice were subjected to TAC for 4 weeks. Interestingly, the K215R mutation in the catalytic site of GRK5 accelerated the decline in cardiac function, as demonstrated by a reduced percentage of EF and FS after TAC compared with WT mice, which also had some reduction post-TAC compared with Sham animals (**Figures 3A and 3B**). Moreover, following chronically elevated afterload, GRK5-K215R mice also presented an augmented dilation of cardiac chambers (left ventricular internal diameter at end diastole) (**Figure 3C**) and increased cardiac hypertrophy and fibrosis compared with sham groups (**Figures 3D and 3E**). However, after TAC in GRK5-K215R hearts, cardiac fibrosis rates were higher than those observed in TAC hearts from WT mice.

NUCLEAR GRK5 SERVES AS A CRITICAL P53 REGULATOR IN VITRO. To further assess the mechanism by which GRK5 regulates the cardiac p53 expression and then apoptosis, we transduced H9c2 cardiomyoblasts with Adenoviruses (Ad), expressing either WT GRK5 or a mutant that renders GRK5 incapable of translocating to the nucleus (ΔNLS)[7] (**Figures 4A and 4B**). As a control, we employed an AD encoding for GFP (**Figure 4B**). When GRK5 elevation was confined outside the nucleus, p53 protein (**Figure 4B**) and mRNA (**Figure 4C**) expression was markedly lower. In contrast, no difference among the groups was observed in terms of cleaved caspase 3 (CC3) and NF-kB p65 phosphorylation (pp65) levels (**Figures 4D and 4E**), suggesting that cytosolic and membrane GRK5 activity were not involved in noxious effects attributed to this kinase. Thus, to explore the role of nuclear GRK5, we next transfected H9c2 cells with a plasmid expressing a mutant GRK5 with a mutation of its nuclear export signal that cannot escape

the nucleus (ΔNES)[6] (Figure 5A). Notably, when GRK5 was trapped in the nucleus, the expression of p53 was significantly increased compared with the control cells (empty plasmid) (Figures 5B and 5C). Analogously, in ΔNES cells, we observed augmented levels of both CC3 and pp65 (Figures 5D and 5E).

To test the relevance of increased p53 expression for GRK5-K215R effects, we employed the p53-inhibitor compound PIFα. As shown in Supplemental Figure 6, to test the efficacy of p53 inhibition, we pretreated H9c2 cells with PIFα (20 μmol/L) for 2 hours,[28] then we stimulated the cells with doxorubicin (DOXO, 0.5 μmol/L), a well-recognized activator of p53, for 24 hours. Of note, as expected, DOXO resulted in a robust increase in p53 expression, and PIFα significantly abolished the effects of DOXO.

Next, we treated H9c2 cells expressing the GRK5 mutant ΔNES with PIFα for 2 hours. Then after 24 hours, we assessed the effects on p53 and apoptosis (Figures 5F and 5G). Notably, PIFα prevented p53 upregulation and markedly abolished the apoptotic response in ΔNES compared with control cells (Figures 5F and 5G).

These results suggest that the expression/activity of p53 by GRK5 is predominantly controlled at the nuclear level and at least in part is caused by the direct effects that GRK5 elicits at the DNA level, as previously reported.[6] In fact, Johnson et al[6] demonstrated that GRK5 binds DNA in vitro, and for this ability, the intact NLS is required.

Then, to validate and expand the view outlined in the previous text using CRISP/Cas9 technology, we generated a stable cell line (using 3T3 cells) expressing the GRK5-K215R mutant protein. In these cells, we confirmed that in the presence of K215R mutation, GRK5 lost its ability to transactivate and then induce the phosphorylation of the EGFR and ERK MAPK in response to Iso administration (Supplemental Figure 7). The analysis of nuclear extracts from both WT and K215R cells did not significantly differ in terms of the nuclear localization of GRK5 (Figure 6A). However, a DNA binding assay revealed that the K215R mutant binds DNA more avidly than the WT GRK5 protein (Figure 6B). Next, the cells were transduced with Adeno-Gq-CAM, which encodes a constitutively active mutant (CAM) of Gαq that, as previously shown by us,[7] induces the translocation of GRK5 into the nuclei (Supplemental Figure 8). As control a group of cells was transduced with an AD encoding for LacZ. Interestingly, in the presence of Gq-CAM, p53 expression was significantly increased in WT cells compared with control cells (Figure 6C). Of note, K215R cells (LacZ and Gq-CAM expressing) presented with levels of p53 that were similar to those observed in WT cells expressing Gq-CAM. Next, we analyzed the impact of the mutant protein on cell survival and whether these were dependent by p53. Our results demonstrated that PIFα protected K215R cells, preventing both the activity of Caspase-3 (Figure 6D) and the apoptotic response (Figure 6E).

NUCLEAR GRK5 DIRECTLY REGULATES FIBROSIS, PROMOTING THE TRANSITION OF FIBROBLASTS INTO MYOFIBROBLASTS IN A KINASE-INDEPENDENT MANNER. Previous studies from our group have shown that GRK5 is a direct regulator of fibroblast function.[12] In particular, in the nucleus of these cells, GRK5 has been shown to promote the transition into activated myofibroblasts in the heart, which are typically involved in maladaptive cardiac remodeling and progressive functional decline.[29] Thus, to address this critical point, we evaluated the effects of K215R mutation on the phenotype of 3T3 fibroblasts. As shown in Figures 7A and 7B, we observed that K215R cells present increased αSMA-2 actin expression. Subsequently, WT fibroblasts were transduced with Ad-Gq-CAM. In these cells, we observed that Gq-CAM expression was accompanied to an increased expression of αSMA, compared with WT cells expressing LacZ as control subjects (Figure 7C). Notably, in K215R cells we observed that αSMA levels were similarly upregulated in both LacZ and Gq-CAM-expressing cells, supporting the central role of GRK5 in regulating cardiac fibrosis.

DISCUSSION

GRK5 is a multifunctional protein with several protein domains, each conferring to this protein the ability to interact with GPCRs and non-GPCR-related signaling molecules, depending on subcellular location and/or specific stimuli. For instance, GRK5 possesses an NLS and NES; thus, it can move inside and outside of the nucleus in response to certain conditions.[19] In addition, data from our laboratory and others suggest that GRK5 can directly bind specific transcriptional active DNA motifs,[6,9] thus strengthening the hypothesis of a novel role for GRK5 in the nucleus. For these reasons, there is a keen interest in determining the proper physiological and pathological roles of GRK5. Moreover, a better understanding of whether and how its kinase activity directly impacts non-GPCR targets, especially nuclear targets such as DNA, is needed. Addressing these questions may shed light on the best way to therapeutically target GRK5 to block this kinase's noxious effects that have been seen in diseases such as HF[1,30] or promote its protective effects that have also been noted.[5]

Accordingly, we generated novel knock-in mice in this study where all endogenous GRK5 was mutated (K215R) to be catalytically inactive. Interestingly, GRK5-K215R mice were found to have significant cardiac dysfunction in young (4 weeks of age) and in adulthood (9-10 weeks of age) with high levels of cardiac cell apoptosis and fibrosis compared with WT littermates. Indeed, the loss of cells in the heart with replacement fibrosis could explain the loss of contractile force and dilatation observed via echocardiography. In vivo, all of these effects translated into increased susceptibility to stress such as LV pressure overload, because GRK5-K215R mice had a heightened pathological response to TAC with even more dysfunction that included fibrosis.

Higher levels of apoptosis in the hearts of these mutant mice were corroborated with higher levels of proapoptotic genes expression and particularly of p53. Thus, the net effect is increased cell death in the heart with replacement fibrosis seen basally and after TAC-induced stress and appears to be mechanistically involved in the significant cardiac dysfunction seen in our mouse model with catalytical inactive GRK5 replacing WT expression. Moreover, in line with a previous report from our group, our data demonstrated that myocardial fibrosis may occur mainly as follows: 1) in response to cardiomyocytes death; and 2) following the increase in αSMA induced by nuclear GRK5. This latter hypothesis was confirmed with data showing that GRK5 regulates the transition of fibroblasts into myofibroblast.[29] Importantly, our previous data have indicated that these noncanonical GRK5 actions within the nucleus of GRK5 can drive pathological cardiac hypertrophy, fibrosis, and then HF.[7-17,28] Although these include kinase-dependent activities of GRK5 (eg, phosphorylation of HDAC5 and MEF2 de-repression within the nucleus[7,8]), the previously mentioned observation along with previous reports from our and other groups suggest that the pathology of GRK5 may or may not always involve its catalytic activity.[9] Thus, our findings have shown that activity is not needed for GRK5 to up-regulate p53 expression, and the loss of catalytic activity enhances this GRK5-mediated regulation.

Amongst the multiple noncanonical activities of GRK5, the regulation of p53 in tumor cells is one of the more critical reported outside the heart.[18,19,27] For instance, through the inhibition of p53, GRK5 confers protection against DNA damage and p53-mediated apoptosis.[18,27] Whether and how the nuclear activity of GRK5 in cardiomyocytes is also related to p53 regulation was unknown. However, our findings that GRK5-K215R hearts had more apoptosis are even more intriguing, consistent with GRK5 playing a role in modulating p53-mediated cell death in myocardial cells. In particular, the demonstration that ΔNES mutant of GRK5, confined in the nucleus, leads to the most significant p53 expression/activity with consequent increased apoptosis adds considerably to the understanding of GRK5's nuclear role. All of these data have a tremendous effect if we consider that as in cancer cells, in presence of p53 inhibitor, nuclear GRK5 lost its proapoptotic role.

Further, in vitro in 3T3 cells, we corroborated the previous observation suggesting that GRK5 bind the DNA more avidly when its catalytic domain is depleted. Indeed, the K215R mutation positively affected the DNA-binding ability of GRK5, but did not influence the subcellular localization. Most importantly, associated with this effect, we observed a robust increase in p53 expression with an augmented CC3 levels and apoptotic response. These effects were completely abolished by p53-inhibitor PIFα.

Overall, our data support, at least in part, the pathological basal phenotype observed in K215R mice and a role for GRK5's kinase activity in controlling normal cardiac function. Of note, it was astounding to observe a lack of effects of GRK5-K215R on hypertrophy. However, as previously shown by us,[7] GRK5-dependent hypertrophy is determined primarily on its ability to phosphorylate HDAC5 and induce MEF2 activity. Although our group has previously demonstrated that GRK5 induces hypertrophy via NFATc3-enhanced transcription (via DNA binding), we did not fully explore if this effect required the catalytic domain of the kinase.[9] Moreover, this previously published report did not explore if via DNA-binding GRK5 induced apoptosis. Thus, our study provides crucial new insights on how nuclear GRK5 activity influences myocardial signaling and function, widening the spectrum of the biological actions attributed to this kinase in cardiomyocytes and in noncardiomyocytes. Moreover, because this study suggests a potential beneficial role in cardiomyocyte cell survival both at the plasma membrane via protective signaling through the EGFR and now through p53 suppression in the nucleus (**Figure 8**), perhaps using p53 inhibitors like PIFα or targeting functional domains of GRK5, such as recently down with the Ca^{2+}-CaM domain, to limit nuclear translocation and prevent adverse LV remodeling and cardiac dysfunction[13] would be the best way to offer therapeutic avenues for heart disease.

STUDY LIMITATIONS. First, although we analyzed brain tissue, where GRK5 has a prominent role, the

GRK5-K215R knock-in mice express the mutant GRK5 globally, and we cannot discount that the cardiac phenotype studied is caused by nonmyocyte contributions as demonstrated also by the contribution of fibroblasts. Second, we obtained in vivo data only in 4- and 9- to 10-week-old mice, and it could be essential to assess the impact of the loss of catalytic activity of GRK5 during aging, especially on any potential development of HF. Third, the complete loss of catalytic activity caused by mutation may not mimic a competitive small molecule competitive pharmacological inhibitor that may have therapeutic properties for certain diseases such as heart failure, because not all GRK5 activity would be inhibited with such agents. Finally, although our preliminary data suggest that GRK5 can act as a transcriptional regulator of p53, we did not assess if GRK5 binds to a specific DNA-regulatory sequence within the p53 genes or other genes. For instance, direct binding of GRK5 should be measured by ChIP-Seq assay. This should be an important mechanistic data to support the overall hypothesis. However, to our knowledge, no suitable highly selective antibody against GRK5 is available but future attempts with new technology will be interesting to pursue.

CONCLUSIONS

Our study provides crucial new knowledge regarding the biological role of GRK5 in the heart and how this kinase can influence myocardial function. Moreover, since this study suggests that the catalytic activity of GRK5 is needed for survival of myocytes, it demonstrates the importance of future pharmacological strategies directed at GRK5 to limiting this activity. In detail, our study emphasizes that that the primary pathological activity of GRK5 appears to reside when it localizes in the nucleus of cells, especially in myocytes and fibroblasts and the most effective therapeutic agents would be those targeting this compartmentalization.

ACKNOWLEDGEMENT Dr Ying Tian, Temple University, provided the plasmid for CRISPR/Cas9.

FUNDING SUPPORT AND AUTHOR DISCLOSURES

This research was funded by Italian Ministry of Education, Universities and Research "Rita Levi Montalcini 2016" (to Dr Cannavo). The research was also supported by National Institutes of Health grant P01 HL174841 (to Dr Koch), and American Heart Association (Postdoctoral fellowship 17POST33660942 to Dr Lucia). Dr Marzano was supported by a research grant provided by the CardioPaTh PhD program and she was also supported by UniNA and Compagnia San Paolo, in the frame of Programme STAR PLUS. All other authors have reported that they have no relationships relevant to the contents of this paper to disclose.

ADDRESS FOR CORRESPONDENCE: Dr Walter J. Koch, Department of Pharmacology, Center for Translational Medicine, Lewis Katz School of Medicine, Temple University, 3500 North Broad Street, MERB 941, Philadelphia, Pennsylvania 19140, USA. E-mail: walter.koch@temple.edu. OR Dr Alessandro Cannavo, Federico II University of Naples, Department of Translational Medical Sciences, Via S. Pansini, 5, 80131 Naples, Italy. E-mail: alessandro.cannavo@unina.it.

PERSPECTIVES

COMPETENCY IN MEDICAL KNOWLEDGE: HF is the leading cause of morbidity, mortality, and hospitalization in the United States with a prevalence that has increased enormously, and the 5-year survival rate of chronic HF patients remains disappointingly low. The mechanisms leading to pathology are growing in understanding; however, current therapies have a limited impact on pathological growth of the myocardium, either after acute or chronic insults. This study provides crucial new insights on how nuclear GRK5 activity influences myocardial signaling and function widening the spectrum of the biological actions attributed to this kinase. Therefore, GRK5 will be added to the list of factors that are crucial for the development of cardiac decompensation, and by extension, approaches based on GRK5 targeting can be inserted into the therapeutic armamentarium available today.

TRANSLATIONAL OUTLOOK: Despite progress in managing HF, the burden of this syndrome is staggering, with the mortality rate remaining significantly elevated. Although today there is increasing clarity on the mechanisms underlying HF, the therapies currently in use have a limited impact. Therefore, the development of novel therapeutical strategies and the identification of new molecular targets are absolutely needed. This study demonstrates that a single point mutation in the gene encoding for grk5 kinase negatively affects the heart functionality and remodeling. Thus, the translational outlook will be to develop new drugs able to inhibit only the nuclear function of this kinase, which is mostly associated to its noxious effects. Analogously important will be to perform large studies in human evaluating if mutation in the catalytic domain of GRK5 may sensitize subjects to cardiac dysfunction and failure in response to stressors like pressure overload and ischemia. All of these studies will expand our knowledge of pharmacogenomics developing the scientific conclusions for selected gene-drug interactions toward personalized medicine.

REFERENCES

1. Sato PY, Chuprun JK, Schwartz M, Koch WJ. The evolving impact of g protein-coupled receptor kinases in cardiac health and disease. *Physiol Rev*. 2015;95(2):377–404.

2. Cannavo A, Komici K, Bencivenga L, et al. GRK2 as a therapeutic target for heart failure. *Expert Opin Ther Targets*. 2018;22(1):75–83.

3. Colak D, Alaiya AA, Kaya N, et al. Integrated left ventricular global transcriptome and proteome profiling in human end-stage dilated cardiomyopathy. *PLoS One*. 2016;11(10):e0162669.

4. Dzimiri N, Muiya P, Andres E, Al-Halees Z. Differential functional expression of human myocardial G protein receptor kinases in left ventricular cardiac diseases. *Eur J Pharmacol*. 2004;489(3):167–177.

5. Noma T, Lemaire A, Naga Prasad SV, et al. Beta-arrestin-mediated beta1-adrenergic receptor transactivation of the EGFR confers cardioprotection. *J Clin Invest*. 2007;117(9):2445–2458.

6. Johnson LR, Robinson JD, Lester KN, Pitcher JA. Distinct structural features of G protein-coupled receptor kinase 5 (GRK5) regulate its nuclear localization and DNA-binding ability. *PLoS One*. 2013;8(5):e62508.

7. Martini JS, Raake P, Vinge LE, et al. Uncovering G protein-coupled receptor kinase-5 as a histone deacetylase kinase in the nucleus of cardiomyocytes. *Proc Natl Acad Sci U S A*. 2008;105(34):12457–12462.

8. Gold JI, Martini JS, Hullmann J, et al. Nuclear translocation of cardiac G protein-Coupled Receptor kinase 5 downstream of select Gq-activating hypertrophic ligands is a calmodulin-dependent process. *PLoS One*. 2013;8(3):e57324.

9. Hullmann JE, Grisanti LA, Makarewich CA, et al. GRK5-mediated exacerbation of pathological cardiac hypertrophy involves facilitation of nuclear NFAT activity. *Circ Res*. 2014;115(12):976–985.

10. Cannavo A, Liccardo D, Eguchi A, et al. Myocardial pathology induced by aldosterone is dependent on non-canonical activities of G protein-coupled receptor kinases. *Nat Commun*. 2016;7:10877.

11. Traynham CJ, Cannavo A, Zhou Y, et al. Differential role of g protein-coupled receptor kinase 5 in physiological versus pathological cardiac hypertrophy. *Circ Res*. 2015;117(12):1001–1012.

12. Eguchi A, Coleman R, Gresham K, et al. GRK5 is a regulator of fibroblast activation and cardiac fibrosis. *Proc Natl Acad Sci U S A*. 2021;118(5):e2012854118.

13. Coleman RC, Eguchi A, Lieu M, et al. A peptide of the N terminus of GRK5 attenuates pressure-overload hypertrophy and heart failure. *Sci Signal*. 2021;14(676):eabb5968.

14. de Lucia C, Grisanti LA, Borghetti G, et al. GRK5 contributes to impaired cardiac function and immune cell recruitment in post-ischemic heart failure. *Cardiovasc Res*. 2021:cvab044.

15. Yi XP, Gerdes AM, Li F. Myocyte redistribution of GRK2 and GRK5 in hypertensive, heart-failure-prone rats. *Hypertension*. 2002;39(6):1058–1063.

16. Yi XP, Zhou J, Baker J, Wang X, Gerdes AM, Li F. Myocardial expression and redistribution of GRKs in hypertensive hypertrophy and failure. *Anat Rec A Discov Mol Cell Evol Biol*. 2005;282(1):13–23.

17. Oda T, Yamamoto T, Kato T, et al. Nuclear translocation of calmodulin in pathological cardiac hypertrophy originates from ryanodine receptor bound calmodulin. *J Mol Cell Cardiol*. 2018;125:87–97.

18. Chen X, Zhu H, Yuan M, Fu J, Zhou Y, Ma L. G-protein-coupled receptor kinase 5 phosphorylates p53 and inhibits DNA damage-induced apoptosis. *J Biol Chem*. 2010;285(17):12823–12830.

19. Marzano F, Rapacciuolo A, Ferrara N, Rengo G, Koch WJ, Cannavo A. Targeting GRK5 for treating chronic degenerative diseases. *Int J Mol Sci*. 2021;22(4):1920.

20. Islam KN, Bae JW, Gao E, Koch WJ. Regulation of nuclear factor κB (NF-κB) in the nucleus of cardiomyocytes by G protein-coupled receptor kinase 5 (GRK5). *J Biol Chem*. 2013;288(50):35683–35689.

21. Sorriento D, Ciccarelli M, Santulli G, et al. The G-protein-coupled receptor kinase 5 inhibits NFkappaB transcriptional activity by inducing nuclear accumulation of IkappaB alpha. *Proc Natl Acad Sci U S A*. 2008;105(46):17818–17823.

22. Zhang Lab guide design resources. Accessed January 10, 2022. http://crispr.mit.edu/

23. Willets JM, Challiss RA, Nahorski SR. Endogenous G protein-coupled receptor kinase 6 Regulates M3 muscarinic acetylcholine receptor phosphorylation and desensitization in human SH-SY5Y neuroblastoma cells. *J Biol Chem*. 2002;277(18):15523–15529.

24. Sato PY, Chuprun JK, Grisanti LA, et al. Restricting mitochondrial GRK2 post-ischemia confers cardioprotection by reducing myocyte death and maintaining glucose oxidation. *Sci Signal*. 2018;11(560):eaau0144.

25. Zhang C, Liu R, Yuan J, et al. Predictive values of N-terminal pro-B-type natriuretic peptide and cardiac troponin I for myocardial fibrosis in hypertrophic obstructive cardiomyopathy. *PloS One*. 2016;11:e0146572.

26. Walther T, Klostermann K, Heringer-Walther S, Schultheiss HP, Tschöpe C, Stepan H. Fibrosis rather than blood pressure determines cardiac BNP expression in mice. *Regul Pept*. 2003;116(1-3):95–100.

27. Michal AM, So CH, Beeharry N, et al. G Protein-coupled receptor kinase 5 is localized to centrosomes and regulates cell cycle progression. *J Biol Chem*. 2012;287(9):6928–6940.

28. Yang Z, Su Z, DeWitt JP, et al. Fluvastatin prevents lung adenocarcinoma bone metastasis by triggering autophagy. *EBioMedicine*. 2017;19:49–59.

29. Gibb AA, Lazaropoulos MP, Elrod JW. Myofibroblasts and fibrosis: mitochondrial and metabolic control of cellular differentiation. *Circ Res*. 2020;127:427–447.

30. Homan KT, Wu E, Cannavo A, Koch WJ, Tesmer JJ. Identification and characterization of amlexanox as a G protein-coupled receptor kinase 5 inhibitor. *Molecules*. 2014;19(10):16937–16949.

KEY WORDS apoptosis, cardiac, DNA, GRK, nuclear

APPENDIX For an expanded Methods section and supplemental figures, please see the online version of this paper.